AEM
Journals.ASM.org

Cytochrome P450 Initiates Degradation of *cis*-Dichloroethene by *Polaromonas* sp. Strain JS666

Shirley F. Nishino,[a] Kwanghee A. Shin,[a]* James M. Gossett,[b] Jim C. Spain[a]

School of Civil and Environmental Engineering, Georgia Institute of Technology, Atlanta, Georgia, USA[a]; School of Civil and Environmental Engineering, Cornell University, Ithaca, New York, USA[b]

***Polaromonas* sp. strain JS666 grows on *cis*-1,2-dichoroethene (*c*DCE) as the sole carbon and energy source under aerobic conditions, but the degradation mechanism and the enzymes involved are unknown. In this study, we established the complete pathway for *c*DCE degradation through heterologous gene expression, inhibition studies, enzyme assays, and analysis of intermediates. Several lines of evidence indicate that a cytochrome P450 monooxygenase catalyzes the initial step of *c*DCE degradation. Both the transient accumulation of dichloroacetaldehyde in *c*DCE-degrading cultures and dichloroacetaldehyde dehydrogenase activities in cell extracts of JS666 support a pathway for degradation of *c*DCE through dichloroacetaldehyde. The mechanism minimizes the formation of *c*DCE epoxide. The molecular phylogeny of the cytochrome P450 gene and the organization of neighboring genes suggest that the *c*DCE degradation pathway recently evolved in a progenitor capable of degrading 1,2-dichloroethane either by the recruitment of the cytochrome P450 monooxygenase gene from an alkane catabolic pathway or by selection for variants of the P450 in a preexisting 1,2-dichloroethane catabolic pathway. The results presented here add yet another role to the broad array of productive reactions catalyzed by cytochrome P450 enzymes.**

Extensive use of perchloroethene (PCE) and trichloroethene (TCE) as industrial solvents has resulted in soil and groundwater contamination throughout the world (1). Anaerobic bacteria can detoxify PCE and TCE by converting the compounds to ethene (2). Incomplete reduction, however, can lead to accumulation of toxic (*cis*-1,2-dichoroethene [*c*DCE]) and carcinogenic (vinyl chloride [VC]) intermediates in the environment (3) when contaminant plumes migrate into aerobic zones and reductive dehalogenation ceases.

Aerobic bacteria that use VC as a growth substrate are readily isolated from chloroethene-contaminated sites (4). VC (5) and ethene (6) are both assimilated via epoxidation catalyzed by an alkene monooxygenase, followed by conversion of the (chloro)epoxide to a 2-hydroxyalkyl coenzyme M by epoxyalkane coenzyme M transferase. The degradation mechanisms, biochemistry, and genes that encode VC and ethene degradation are analogous for the two compounds (5, 7, 8).

In contrast, *Polaromonas* sp. strain JS666 is the only isolate able to grow with *c*DCE as the sole carbon and energy source (9). *c*DCE degradation is a rate-limiting step in natural attenuation processes for the chlorinated ethenes at many contaminated sites (10, 11). The pathway for *c*DCE biodegradation and the enzymes involved are unknown. The genome of *Polaromonas* sp. strain JS666 contains a number of genes related to metabolism of xenobiotic compounds, but there is no obvious cluster of genes that encode the *c*DCE degradation pathway (12). Whole-genome expression microarrays and protein expression analysis (13) revealed upregulation of genes for enzymes potentially involved in the initial reactions of *c*DCE degradation. They included genes for cyclohexanone monooxygenase, glutathione-*S*-transferase, and cytochrome P450. Genes for (di)chloroacetaldehyde, (di)chloroacetic acid, and (chloro)glycolate transformation were also upregulated in a pattern expected for growth on *c*DCE or 1,2-dichloroethane (DCA). The observations suggested that the *c*DCE and DCA pathways might converge.

Coleman et al. (9) suggested epoxidation as the first step in *c*DCE degradation based on epoxidation of ethene by JS666 after growth on *c*DCE. The epoxidation of chlorinated ethenes by oxygenases is a widespread reaction in bacteria (14–16), but the toxic and highly reactive epoxide intermediates are not assimilated except in the case of VC biodegradation (5). A series of *Escherichia coli* strains with an engineered metabolic pathway for *c*DCE degradation based on epoxide formation and degradation has been constructed. The strains carry combinations of engineered toluene monooxygenase (17) and epoxide hydrolase (18) to catalyze transformation of chloroethenes and up to 4 other engineered proteins to overcome epoxide toxicity (19). Although the strains mineralize *c*DCE, they do not grow on it, and the pathway must be induced with isopropyl-β-D-thiogalactopyranoside.

Many oxygenases, such as the soluble methane monooxygenase from *Methylosinus trichosporium* OB3b (15), produce mixtures of acetaldehydes and epoxides from halogenated ethenes via an intramolecular halogen migration during oxidation. Similarly, in mammalian systems, cytochrome P450 enzymes catalyze the initial attack on chlorinated ethenes to produce a mixture of products. Nonconcerted reactions of human P450 2E1 or rat P450 2B1 oxidize TCE to the corresponding epoxide and 1,1,1-trichloroacetaldehyde (chloral), but the mechanisms controlling the partitioning to the two different intermediates are not fully understood (20).

Here, we describe the initial steps of *c*DCE biodegradation and genes that encode the enzymes involved. The understanding of the

Received 7 November 2012 **Accepted** 21 January 2013
Published ahead of print 25 January 2013
Address correspondence to Jim C. Spain, jspain@ce.gatech.edu.
* Present address: Kwanghee A. Shin, Research Institute of Biotechnology, CJ CheilJedang, Seoul, South Korea.

doi:10.1128/AEM.03445-12

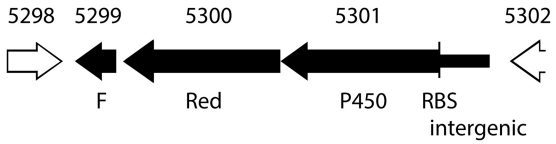

FIG 1 Map of region cloned into pET21a. Key: F, ferredoxin gene; Red, reductase gene; and P450, cytochrome P450 gene. Clones also contain the native ribosome binding site (RBS) and 562 bp of intergenic DNA. Gene loci are indicated above the genes.

*c*DCE degradation pathway will provide the basis to detect, predict, and enhance *c*DCE degradation at contaminated sites as well as increase our understanding of bacterial evolution of catabolic pathways for synthetic chemicals.

MATERIALS AND METHODS

Growth conditions. A 5-liter culture of *Polaromonas* sp. JS666 was routinely grown with *c*DCE as the sole carbon and energy source in a 7-liter bioreactor at 22°C. Minimal salts broth (MSB) (21) was modified as follows: phosphate buffer was 10 mM, and all other nutrients were supplied at half-strength. Neat *c*DCE was continuously supplied via syringe pump (8 to 50 μl/h) to maintain *c*DCE in the culture at 50 to 500 μM. The pH was maintained at 7.0 by the addition of NaOH. Oxygen addition was controlled to maintain dissolved oxygen at 3.5 mg/liter (40% saturation). The reactor was stirred at 400 rpm. Portions of the culture (1 to 2 liters) were harvested by centrifugation and suspended in MSB for use in experiments. Trypticase soy at one-quarter strength solidified with 18 g agar/liter (1/4-TSA) was used to test for the presence of contaminating bacteria. Strain JS666 was also grown in 160-ml serum bottles on half-strength MSB (1/2-MSB) with cyclohexanone (5 mM), glycolate (10 mM), succinate (10 mM), or DCA (0.25 mM) as the carbon source. Inocula were prepared from single colonies grown on agar plates containing cyclohexanone (5 mM) or from cells actively growing on *c*DCE.

Substrate transformation by whole cells. Cells were suspended to an appropriate density (optical densities at 600 nm [OD_{600}], ≈1 for JS666 and 10 to 60 for clones) in 50 ml of 1/2-MSB in 160-ml serum bottles sealed with Teflon-coated butyl rubber stoppers. Reactions were initiated by the addition of substrates, and cultures were incubated at 25°C with shaking (150 rpm). Substrate disappearance and/or product formation was monitored by gas chromatography (GC).

Respirometry. Cells grown on various substrates were harvested by centrifugation, washed with potassium phosphate buffer (pH 7.2; 20 mM), and suspended in the same buffer. Oxygen uptake was measured polarographically at 25°C with a Clark-type oxygen electrode connected to a YSI model 5300 biological oxygen monitor.

Cloning and expression of putative cytochrome P450 monooxygenase. Genomic DNA was extracted with a genomic DNA purification system (Promega, Madison, WI). A 3.5-kb fragment (positions 52538 to 56017 on pPol338; GenBank accession number NC_007950) containing genes encoding the putative cytochrome P450, ferredoxin reductase, ferredoxin, and a 562-bp portion of the intergenic region between the P450 and its upstream neighbor (Bpro_5302; Fig. 1) was amplified by PCR using primers 017F (CACCACGCTGCACCGTGTTATGTTTCAC) and 017R (TCAGTGCTGGCCGAGCGGCG). The PCR mixture (20 μl) contained genomic DNA (50 ng), primers (0.25 μM each), deoxynucleoside triphosphates (0.4 mM each), and Promega GoTaq Hot Start polymerase (2 U) and 1× buffer (Madison, WI). Amplifications (30 cycles) were carried out as follows: 95°C for 1 min, 56°C for 30 s, and 72°C for 1 min, after initial denaturation at 95°C for 10 min. The PCR products were treated with the Klenow fragment of DNA polymerase I (New England BioLabs, MA) and then cloned into the pET101/D-TOPO vector (Novagen, Gibbstown, NJ). The resulting plasmid, designated pJS593, was transformed into *E. coli* BL21 Star(DE3) for expression to create strain JS593.

JS593 was grown in 30 ml of terrific broth medium (TB) containing Overnight Express autoinduction system I (Novagen) at 37°C. When the OD_{600} reached 0.8 to 0.9, the temperature was reduced to 23°C and the cultures were incubated for an additional 14 to 20 h. Cells were harvested by centrifugation, washed twice with phosphate buffer (20 mM, pH 7.5), and stored on ice until used. Improved expression of the insert was obtained when pJS593 was moved into *E. coli* Rosetta 2; the resulting strain was designated JS595. γ-Aminolevulinic acid (0.5 mM) and $FeSO_4$ (0.1 mM) were added at the start of the room temperature incubation (22).

Enzyme assays. Cell extracts were prepared by passing cells twice through a French pressure cell at 20,000 lb/in^2, followed by centrifugation at 160,000 × *g*. Cytochrome P450 monooxygenase activity was assayed by monitoring substrate disappearance (*c*DCE, DCA) and/or product formation by GC. Reaction mixtures (1 ml) consisted of cell extracts (1 to 4 mg protein) and substrates (80 to 160 nmol) in phosphate buffer (50 mM, pH 7.2) in 4-ml bottles sealed with Teflon-coated butyl rubber stoppers. Reactions were started by addition of NADH or NADPH (2.5 mM), and the bottles were incubated at 25°C. At appropriate intervals, the reactions were stopped by the addition of $ZnSO_4$ (30 mM), and the mixtures were extracted with ethyl ether. Aldehyde dehydrogenase (23) was measured by following the reduction of NAD to NADH at 340 nm in the presence of (di)chloroacetaldehyde, cell extract (0.5 to 1 mg protein), and NAD (1 mM). Haloacid dehalogenase (24) was measured by chloride release in the presence of (di)chloroacetate and cell extract (0.5 to 1 mg protein).

Analytical methods. *c*DCE and DCA in headspace samples were monitored with an Agilent 6890N GC equipped with a flame ionization detector (FID) and a Supelco 1% SP-1000 on 60/80 Carbopack B column, 6 ft by 1/8 in. (outer diameter) by 2.1 mm (inner diameter), as previously described (25), with the following modifications. The oven temperature was ramped at 20°C/min from 100°C to 150°C and then at 10°C/min to a maximum of 175°C and held until all compounds eluted. Some samples were spiked with TCE as an internal standard before extraction with ethyl ether. The ether extracts were analyzed by GC or GC-mass spectrometry (MS). Octane was measured in the headspace by GC-FID with a method similar to that for *c*DCE but with a Supelco 10% OV-101 on 80/100 Chromosorb W HP packed glass column, 6 ft by 1/4 in. (outer diameter) by 2 mm (inner diameter). *c*DCE epoxide, dichloroacetaldehyde, and chloroacetaldehyde in ether extracts were analyzed with an HP6890 GC equipped with either an electron-capture detector (ECD) or a 5973 mass detector. Compounds were separated on a DB-5MS column (30 m by 0.25 mm, 0.25-μm film thickness; J&W Scientific, CA). For GC-ECD, the oven temperature was held at 60°C with an injection temperature of 200°C and a detector temperature of 250°C. For GC-MS, the oven temperature was initially held at 35°C for 10 min, ramped at 20°C/min to 175°C, and held at the final temperature for 3 min. Absolute mass determination was performed by the Georgia Institute of Technology Bioanalytical Mass Spectrometry Facility.

Protein was measured with a Pierce bicinchoninic acid protein assay kit (Rockford, IL). Chloride was measured by the method of Bergmann and Sanik (26). Glyoxal was derivatized with 2,4-dinitrophenylhydrazone (27) and then separated on a Phenomenex Synergi Polar-RP column (4 μm; 2.0 mm by 150 mm) with a Varian high-pressure liquid chromatography system equipped with a photodiode array detector. Solid-phase extraction (SPE) was performed with a MEPS C_8 cartridge (SGE, Austin, TX).

Chemicals. *c*DCE (97%, preservative free) was from Sigma-Aldrich. The major contaminant was *trans*-DCE, which was not metabolized by the cultures. All other chemicals were reagent grade. Dichloroacetaldehyde hydrate was converted to dichloroacetaldehyde by the method of Wakasugi (28). *c*DCE epoxide was synthesized chemically (29) and biologically (15) by transformation of *c*DCE by JS593. Products from both methods had the same GC retention times and parent masses [M^+] at *m/z* 112, 114, and 116 which correspond to those of *c*DCE epoxide (30).

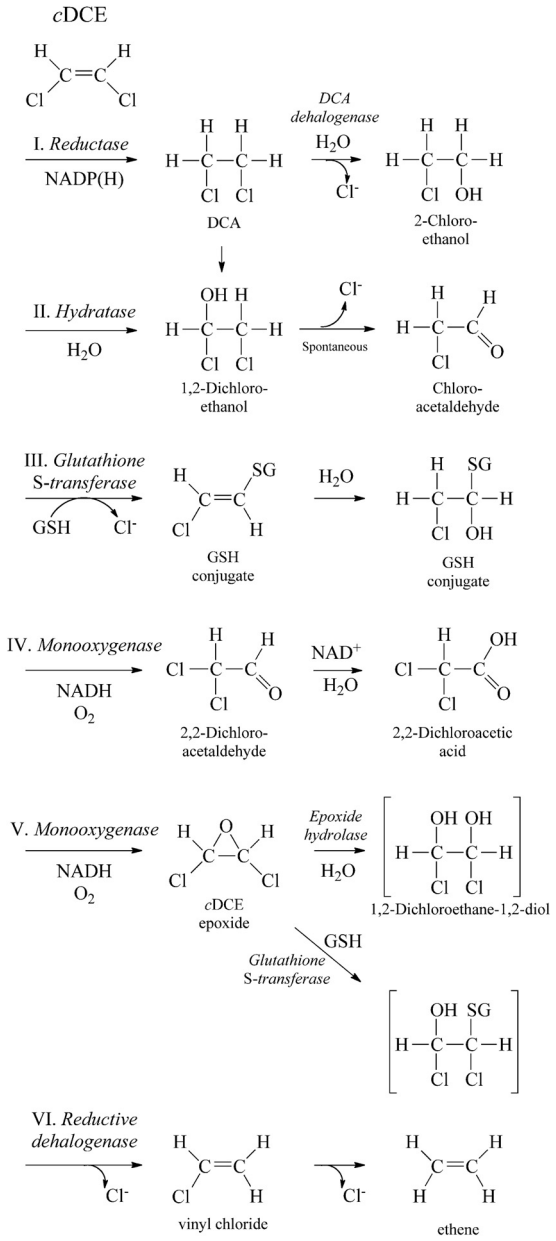

FIG 2 Potential initial steps for *c*DCE degradation in JS666 include reduction (I), hydration (II), glutathione addition (III), monooxygenation to an aldehyde (IV), monooxygenation to an epoxide (V), or reductive dehalogenation (VI). GSH, reduced glutathione; SG, glutathione conjugated to the organic compound, where the H (hydrogen) has been replaced by the organic compound.

RESULTS

Hypothetical initial steps of *c*DCE degradation. We investigated several possible reactions for the initial steps of *c*DCE biodegradation (Fig. 2). A reductase (Fig. 2, pathway I) or hydratase (pathway II) might channel *c*DCE into the DCA degradation pathway (24, 31). Glutathione-*S*-transferase might catalyze formation of glutathione conjugates during *c*DCE biodegradation (pathway III) (13). Monooxygenase enzymes could produce various amounts of an aldehyde (pathway IV) and *c*DCE epoxide (pathway V) (15, 32). Finally, although rare in aerobes, a reductive dehalogenase could catalyze removal of chlorine (pathway VI) (33).

Stimulation of oxygen uptake by potential intermediates of *c*DCE degradation. Respirometry experiments do not provide rigorous conclusions about pathways but allow hypotheses to be made about enzyme induction and involvement of intermediates. The rates reflect not only preferences for the initial substrates but also stoichiometries and kinetics of subsequent reactions along with transport limitations. *c*DCE, DCA, and intermediates of the DCA degradation pathway stimulated oxygen uptake in *c*DCE- and DCA-grown cells of strain JS666 (Table 1). The results indicate (34) that *c*DCE is degraded via DCA or that the *c*DCE and DCA pathways converge. Alternatively, a monooxygenase induced by *c*DCE (13) could transform DCA into chloroacetaldehyde (31). Chloroacetaldehyde might then be degraded by an enzyme that has high constitutive activity but is also moderately upregulated during growth on *c*DCE, DCA, or cyclohexanone (Table 1). Cyclohexanone-grown cells did not oxidize *c*DCE, DCA, or intermediates of the DCA degradation pathway other than choroacetaldehyde, for which there was high constitutive activity in all cells.

Involvement of oxygen in the initial steps of *c*DCE biodegradation. *c*DCE-grown cells required oxygen to metabolize *c*DCE (Fig. 3) and DCA (Fig. 3B). Cell suspensions rapidly transformed *c*DCE and DCA in the presence of oxygen, but no transformation was detected in the absence of oxygen. The result is not consistent with reductase- or hydratase-catalyzed conversion of *c*DCE to DCA. *c*DCE degradation resumed immediately upon addition of air. The results suggest but do not prove that an oxygenase enzyme catalyzes the initial steps in *c*DCE and DCA degradation. The requirement for molecular oxygen also precludes involvement of a reductive dehalogenase.

Metyrapone and phenylhydrazine inhibition of *c*DCE biodegradation. Many cytochrome P450 enzymes are inhibited by metyrapone and phenylhydrazine (35, 36). Both *c*DCE and DCA degradation were inhibited over 90% in intact cells of JS666 by 200 μM metyrapone or phenylhydrazine (Fig. 4A), as measured by either GC or stimulation of oxygen uptake. The oxygen uptake rates with chloroacetaldehyde and cyclohexanone were unchanged. The degree of inhibition of the initial rates of *c*DCE and DCA degradation was proportional to the concentration of metyrapone (Fig. 4B). The results indicate that a cytochrome P450 catalyzes early steps in both *c*DCE and DCA biodegradation in JS666.

***c*DCE degradation kinetics.** Strain JS666 grows on *c*DCE with stoichiometric accumulation of chloride (9). Chloride release was slightly delayed during the early stages of growth of JS666, which suggested a transient accumulation of degradation intermediates. During *c*DCE degradation by JS666 in the present study, small amounts of dichloroacetaldehyde transiently accumulated and then disappeared (data not shown), which suggested strongly that dichloroacetaldehyde is an intermediate of *c*DCE degradation. Trace amounts of *c*DCE epoxide also accumulated in the *c*DCE-degrading cultures. The detection of dichloroacetaldehyde and *c*DCE epoxide in *c*DCE-degrading cultures is consistent with the involvement of the cytochrome P450 monooxygenase, here called *c*DCE monooxygenase, in the initial steps of *c*DCE degradation in JS666.

Cloning and expression of *c*DCE monooxygenase. Four genes are annotated as cytochrome P450 in the genome of JS666.

TABLE 1 Oxygen uptake by resting cells of JS666[a]

Test substrate (concn [mM])	Oxygen uptake (nmol min^{-1} mg^{-1} protein) after growth on:				
	*c*DCE	DCA	Cyclohexanone	Glycolate	Succinate
*c*DCE (1.0)	13 ± 0	6 ± 2	<1	<1	<1
1,2-DCA (1.0)	11 ± 0	23 ± 6	<1	<1	<1
2-Chloroethanol (1.0)	7 ± 2	13 ± 0	<1	<1	<1
Chloroacetaldehyde hydrate (0.5)	55 ± 1	47 ± 0	81 ± 6	39 ± 2	27 ± 5
Dichloroacetaldehyde hydrate (0.5)	18 ± 2	12 ± 0	6 ± 4	7 ± 1	3 ± 0
Cyclohexanone (0.5)	10 ± 1	1 ± 2	276 ± 36	<1	<1
Chloroacetate (1.0)	2 ± 0	26 ± 8	<1	7 ± 2	2 ± 1
Dichloroacetate (1.0)	ND	10 ± 3			
Glycolate (1.0)	7 ± 2	14 ± 2	<1	95 ± 1	6 ± 2
Succinate (1.0)		7 ± 1	32 ± 1		41 ± 1

[a] Oxygen uptake by resting cells of JS666 grown with various substrates. Reaction mixtures contained substrate, cells (0.29 to 0.31 mg of protein), and air-saturated phosphate buffer (20 mM, pH 7.2) to a final volume of 1.85 ml. *c*DCE, 1,2-DCA, and cyclohexanone were added from a 1.0 M stock in acetone, and the other substrates were dissolved in water. Acetone did not affect the rates of oxygen uptake. Data represent means and standard deviations from at least two measurements. ND, not determined; blank cell, not tested.

Bpro_5301, which was upregulated 3.5-fold by growth on *c*DCE (13), is located on pPol338, the smaller of two megaplasmids in JS666. Bpro_5301 is adjacent to genes annotated as flavin adenine dinucleotide-dependent pyridine nucleotide disulfide oxidoreductase (Bpro_5300) and ferredoxin (Bpro_5299). The amino acid sequence of the cytochrome P450 is 76% identical to that of alkane hydroxylase (AphG) from *Mycobacterium* sp. strain HXN-1500, while the amino acid sequences of the oxidoreductase (AphH) and ferredoxin (AphI) are each 66% identical to the sequences from HXN-1500 (12, 37). AphH and AphI of HXN-1500 are the most closely related to the proteins of JS666 of any currently entered in GenBank. The three genes from JS666 were cloned together into *E. coli* (Fig. 1), and the expression of each component was confirmed by SDS-PAGE (Fig. 5). JS593 catalyzed the transformation of DCA and *c*DCE at 1.0 and 0.2 nmol/min/mg protein, respectively. No transformation of *c*DCE or DCA was observed in the absence of oxygen, but transformation was immediate upon the addition of

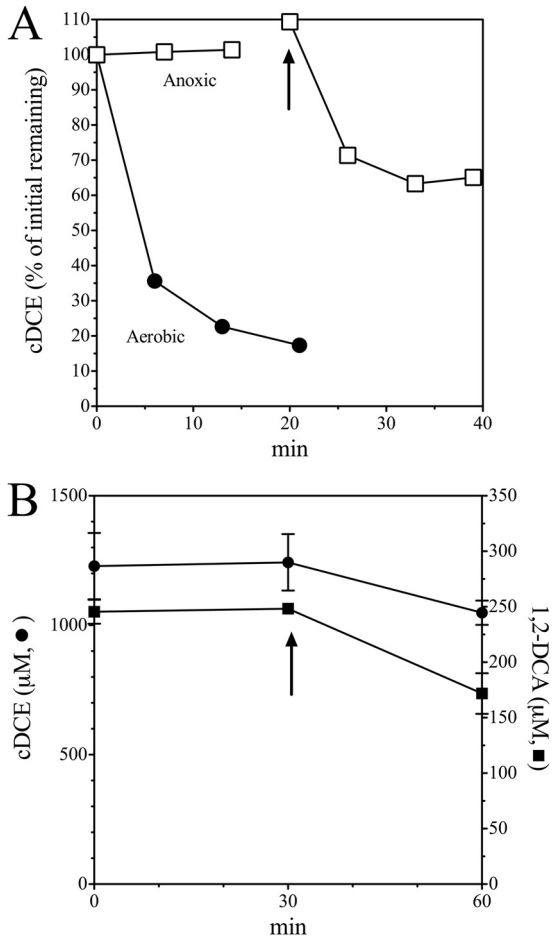

FIG 3 Dependence of *c*DCE and DCA degradation by JS666 on oxygen. (A) *c*DCE-grown cells were added to N_2-sparged (□) and unsparged (●) serum bottles. Reactions were initiated by addition of *c*DCE to the bottles. Arrow, addition of 5 ml of air. (B) *c*DCE and DCA were added as neat solutions to N_2-sparged serum bottles. Reactions were initiated by adding 1 ml of *c*DCE-grown sparged cells to bottles. Arrow, addition of 1 ml of O_2. Error bars indicate 1 standard deviation.

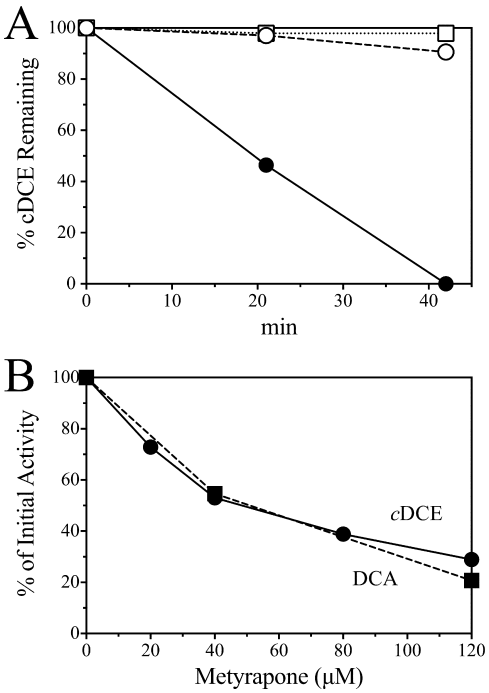

FIG 4 Effect of cytochrome P450 inhibitors on JS666. (A) Time course of *c*DCE degradation with no inhibitor (●), 200 μM metyrapone (○), or 200 μM phenylhydrazine (□). (B) Concentration-dependent effect of metyrapone on *c*DCE (●) and DCA (■) degradation by JS666. *c*DCE and DCA were provided at 100 μM.

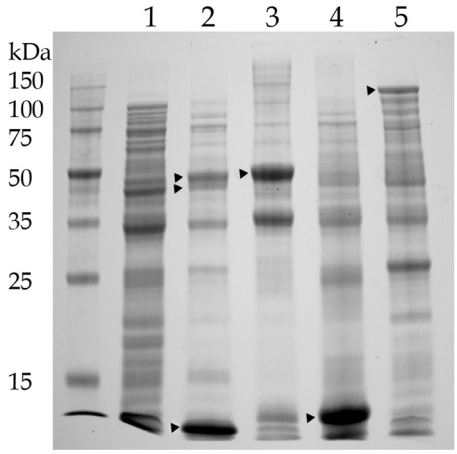

FIG 5 Expression of cytochrome P450. Lane 1, uninduced clone; lane 2, induced clone expressing Bpro_5301 (47.49 kDa), Bpro_5300 (43.18 kDa), and Bpro_5299 (11.29 kDa); lane 3, clone expressing Bpro_5301 with a 6× His tag (48.32 kDa); lane 4, clone expressing Bpro_5299 with a 6× His tag (12.12 kDa); lane 5, clone expressing LacZ (120 kDa).

oxygen. *E. coli* containing the pET vector alone did not catalyze transformation of any of the substrates.

Products of transformation of *c*DCE by *c*DCE monooxygenase. Resting cells of *E. coli* JS595 catalyzed the transformation of *c*DCE to 2,2-dichloroacetaldehyde (up to 88%; mean = 61% ± 12%, $n = 12$), accompanied by the appearance of an unidentified metabolite in the headspace. In preliminary experiments (Fig. 6), the recovery of 2,2-dichloroacetaldehyde was modest because the compound partitioned to the cells. In subsequent experiments that included multiple extractions with the cells included in the extraction, recovery of dichloroacetaldehyde improved. The rate of transformation of *c*DCE by JS593 or JS595 rapidly diminished so that it was only a fraction of the initial rate after 30 to 60 min. The production of dichloroacetaldehyde also diminished rapidly, while the unidentified metabolite continued to accumulate, which suggested that it resulted from abiotic transformation of 2,2-dichloroacetaldehyde. When JS666 was grown on *c*DCE, no dichloroacetaldehyde accumulated and only traces of the unknown metabolite were detected in the headspace (Fig. 6). The unidentified metabolite was never found in extracts of the aqueous phase, nor was it metabolized by JS666. The unidentified metabolite appeared as a major peak by GC-ECD but was undetectable by GC-FID and was barely detectable by GC-mass selection detector (MSD). The mass spectrum (Fig. 6B) did not match that of any of the known metabolites of chloroethenes/ethanes, although the exact mass was 112. Because the mass balance with JS595 cells and cell extracts of JS593 and JS595 indicated that *c*DCE is predominantly transformed into dichloroacetaldehyde and the wild type accumulates only traces of the unknown metabolite, attempts to identify the unknown were discontinued.

Traces of *c*DCE epoxide occasionally accumulated in *c*DCE-degrading cultures, but lack of a published extinction coefficient prevented quantitation of the epoxide. The results indicate that *c*DCE monooxygenase specifically transforms *c*DCE mainly to dichloroacetaldehyde rather than to epoxide. They also indicate that other enzymes in JS666 but not in *E. coli* prevent the accumulation of dichloroacetaldehyde and the unknown metabolite.

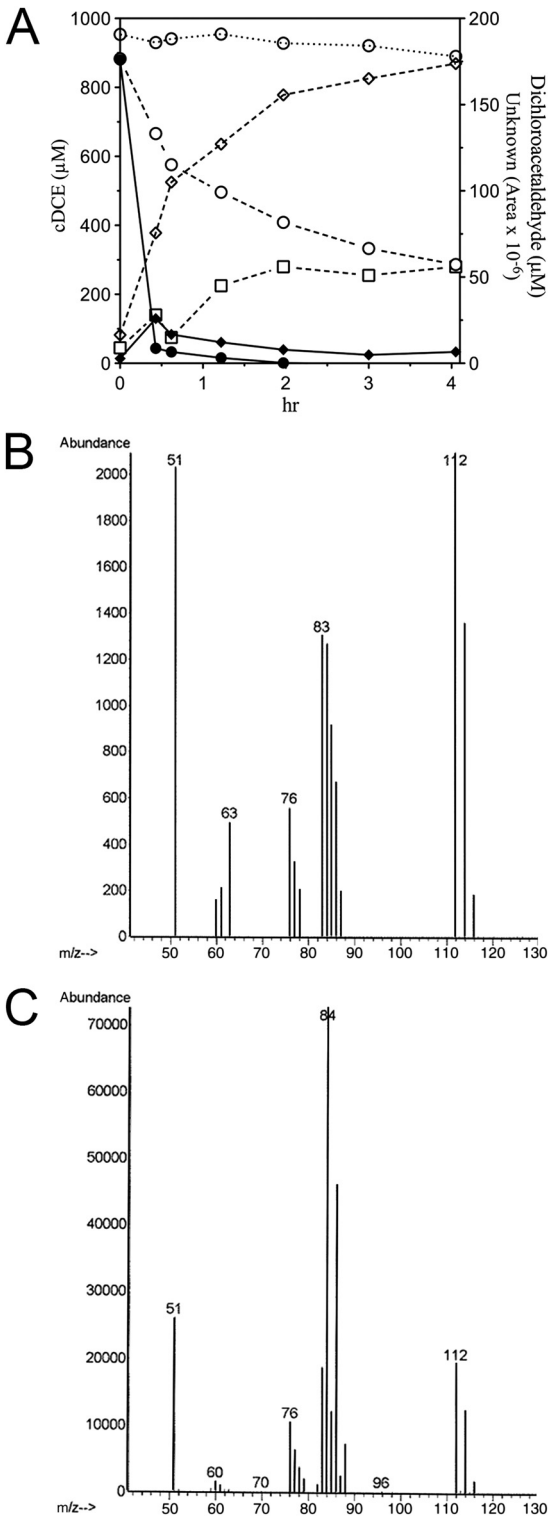

FIG 6 (A) Degradation of *c*DCE by JS666 (solid lines and symbols; $OD_{600} \approx 1$) and transformation by JS595 (dashed lines, open symbols; $OD_{600} \approx 40$) and uninoculated control (open circle, dotted line). Circles, *c*DCE; squares, 2,2-dichloroacetaldehyde; diamonds, unknown metabolite. (B) Mass spectrum of unknown. (C) Mass spectrum of 2, 2-dichloroacetaldehyde.

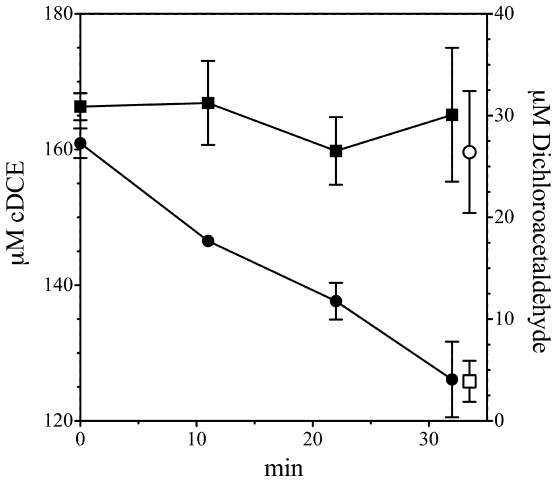

FIG 7 Biotransformation of *c*DCE in cell extracts of JS595 expressing *c*DCE monooxygenase. Complete mixtures contained *c*DCE, phosphate buffer, cell extract, and NADH. Controls lacked either NADH or cell extract. Results are for *c*DCE in complete mixtures (●), *c*DCE in controls (■), final dichloroacetaldehyde in complete mixtures (○), and final dichloroacetaldehyde in controls (□). *c*DCE was allowed to equilibrate for 5 min, and then reactions were initiated by adding NADH.

Dichloroacetaldehyde production in cell extracts of JS593 and JS595. Dichloroacetaldehyde was produced during *c*DCE transformation by extracts prepared from cells of JS593 or JS595 (Fig. 7). With dialyzed extracts, the reaction took place only when NADH was present in the reaction mixture. When DCA was the substrate, chloroacetaldehyde was produced. The enzyme activity was modest and unstable, but the results were reproducible. The results indicate that the *c*DCE monooxygenase catalyzes the transformation of both *c*DCE and DCA to chloroacetaldehydes that can be further degraded in JS666.

Dichloroacetaldehyde transformation in cell extracts of JS666. Dichloroacetaldehyde was degraded at a rate of 15.6 nmol min^{-1} mg^{-1} protein in extracts of cells grown on *c*DCE (Table 2), which is consistent with the rate of *c*DCE degradation by whole cells (17 nmol min^{-1} mg^{-1} protein). The apparent K_m of the dichloroacetaldehyde dehydrogenase was 120 ± 12 μM. Genes that encode dichloroacetaldehyde dehydrogenase were not identified experimentally. There are several potential candidates for the genes that encode chloroacetaldehyde dehydrogenase and dichloroacetaldehyde dehydrogenase, but we do not have sufficient evidence from microarray data to establish which ones encode the activities that we measured in cells and cell extracts. The haloacid dehalogenase upregulated by *c*DCE catalyzes transformation of (di)chloroacetic acid (13, 64), and (di)chloroacetic acid was transformed in cell extracts of JS666 (Table 2). The results indicate that *c*DCE degradation via dichloroacetaldehyde is the productive pathway in JS666.

TABLE 2 Enzyme activities measured in cell extract of *Polaromonas* sp. JS666

Enzyme assayed	Substrate	Sp act[a] (nmol min^{-1} mg^{-1} protein)
Aldehyde dehydrogenase	Dichloroacetaldehyde	15.6 ± 0.1
	Chloroacetaldehyde	24.8 ± 5.2
Haloacid dehalogenase	Dichloroacetate	15.0 ± 2.8
	Chloroacetate	10.3 ± 1.6

[a] Data represent means and standard deviations from at least two measurements.

TABLE 3 Transformation of alkanes by cytochrome P450[a]

Substrate	Product(s)	Sp act (nmol min^{-1} mg^{-1} protein)	
		Replicate 1	Replicate 2
cDCE	Dichloroacetaldehyde	0.39	0.26
Hexane	1-Hexanol	0.005	0.01
Cyclohexane	Cyclohexanol	0.07	0.10
Octane	1-Octanol, 2-octanol, 2-octanone	0.07	0.06
Limonene	Perillyl alcohol, 2 unidentified peaks	0.06	0.08

[a] *E. coli* JS595 was provided with *c*DCE or alkane. Products were extracted and analyzed by GC-MS.

Transformation of alkanes by *c*DCE monooxygenase. Bpro_5301 is most closely related to a gene encoding a medium-chain alkane hydroxylase and was previously shown to enable the catalysis of *n*-alkanes to primary alcohols (38). Various alkanes were transformed by *E. coli* JS595 (Table 3). The rate of transformation of *c*DCE was an order of magnitude faster than the rates of transformation of the alkanes. The primary alcohols expected as the products of the alkane transformation (38, 39) were detected in SPE extracts of all cultures by GC-MS and were the only products of hexane and cyclohexane transformation. 2-Octanol and 2-octanone were detected in octane transformations along with the major 1-octanol peak. Perillyl alcohol was the major product of limonene transformation but was accompanied by two other unidentified peaks. The results indicate that although *c*DCE monooxygenase can still transform *n*-alkanes, it appears to be specialized for *c*DCE.

DISCUSSION

Several lines of evidence indicate that *c*DCE monooxygenase is responsible for the initial steps in *c*DCE biodegradation in JS666. *c*DCE was degraded only in the presence of oxygen, degradation was inhibited by cytochrome P450-specific inhibitors, heterologously expressed cytochrome P450 monooxygenase catalyzes the transformation of *c*DCE to dichloroacetaldehyde, and Bpro_5301 is upregulated by *c*DCE (13). The transient accumulation of dichloroacetaldehyde in *c*DCE-degrading cultures and the dichloroacetaldehyde dehydrogenase activities in cell extracts of JS666 support the proposed pathway (Fig. 8). Transformation of dichloroacetaldehyde and dichloroacetate in cell extracts of JS666 (Table 2) supports a downstream pathway of *c*DCE degradation similar to that of 1,2-dichloroethane (Fig. 8). Chloroglycolate would be expected to spontaneously dechlorinate to glyoxalate (40). The ability of JS666 to metabolize glyoxalate is inferred from the growth of JS666 on glycolate and the presence of putative glyoxalate pathway genes encoding isocitrate lyase (Bpro_2101) and malate synthase (Bpro_4517).

*c*DCE monooxygenase is also responsible for initiation of DCA degradation. Genes that encode the enzymes of the DCA degradation pathway are expressed in cells of JS666 grown on *c*DCE (13, 24), and clones that catalyzed the transformation of *c*DCE also catalyzed the transformation of DCA. The inhibition of DCA degradation by metyrapone in cells grown on DCA, the transformation of DCA to chloroacetaldehyde by *c*DCE monooxygenase, and

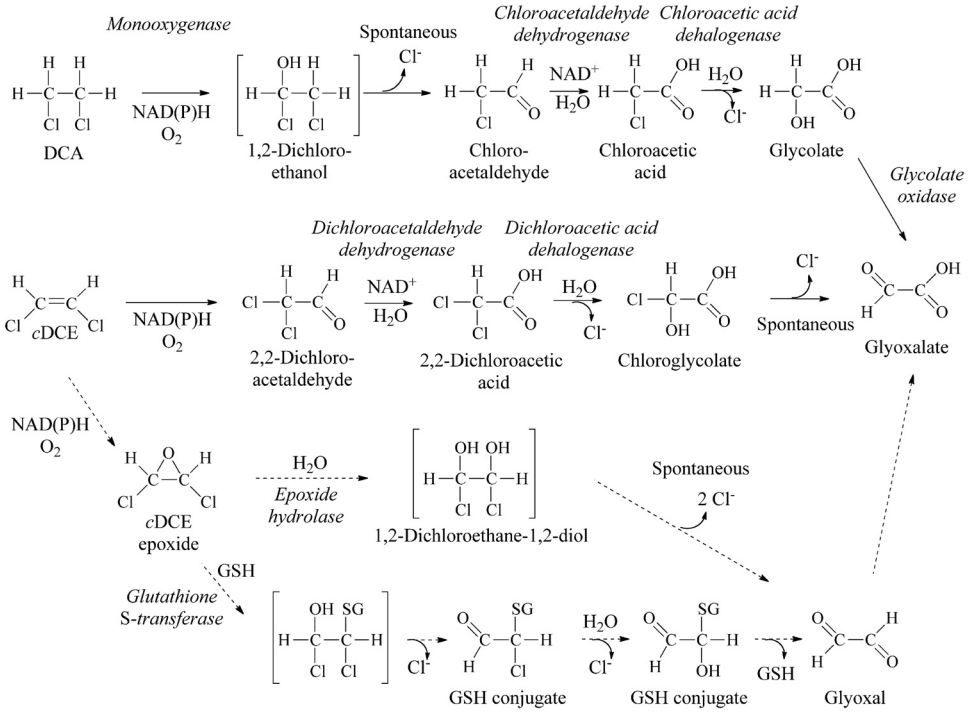

FIG 8 Proposed *c*DCE and DCA degradation pathways. Solid arrows, major pathways supported by the results of this study; dashed arrows, potential minor pathways.

the failure to transform DCA in the absence of oxygen support the hypothesis that strain JS666 degrades DCA by an oxidative pathway (Fig. 8).

JS666 could grow only on low concentrations of DCA (100 to 200 μM), which is consistent with previous studies indicating that JS666 could not grow on 200 μM to 10 mM DCA (9, 12). Although the same genes are responsible for *c*DCE and DCA degradation, growth on DCA is limited to concentrations an order of magnitude less than concentrations that support growth on *c*DCE. A contributing factor possibly lies in the greater solubility of DCA in the aqueous phase. It is also possible that chloroacetaldehyde is more toxic to JS666 than dichloroacetaldehyde.

The degradation of DCA has been most extensively studied in *Xanthobacter autotrophicus* GJ10 (24). The strain constitutively expresses two different dehalogenases; however, the hydrolytic pathway (Fig. 2, pathway II) in strain GJ10 is inconsistent with the results from JS666. *Pseudomonas* sp. strain DE2 (41) and *Pseudomonas* sp. strain DCA1 (31) degrade DCA by the oxidative pathway proposed for degradation of DCA by JS666 (Fig. 8). The monooxygenase from DE2 and DCA1 has not been identified. It seems likely that the reaction might be catalyzed by a P450 monooxygenase similar to the *c*DCE monooxygenase. Sequence information is not available for strain DE2 or DCA1, so the relatedness of the enzymes is unknown. It is known, however, that strain DCA1 transforms *c*DCE after growth on DCA (31).

Monooxygenation of *c*DCE and DCA by the same enzyme in JS666 thus accounts for the results of the simultaneous adaptation studies as well as for why *c*DCE degradation is induced in DCA-grown cells. The regulation of the metabolic pathway, however, is not understood. It seems likely that the regulation is in the early stages of evolution, as evidenced by long and unpredictable acclimation periods when cells are switched from more favored substrates to *c*DCE.

Cytochrome P450-catalyzed oxidation of chlorinated ethenes can yield multiple products. The formation of chloroacetaldehydes during the oxidation of 1,1-dichloroethene (42) and trichloroethene (32) by cytochromes P450 from rat liver microsomes has been reported. A transient chloroethene intermediate bound in the cytochrome P450 can be partitioned to epoxide, a chloroacetaldehyde via chloride migration, and a dead-end product due to an irreversible porphyrin *N*-alkylation (32, 43, 44). Theoretical studies on terminal olefin oxidation by cytochrome P450 suggest that different environments in the protein pocket of the enzyme may lead to different product ratios of epoxides, aldehydes, and suicide products (44). The mass balance derived from the studies with intact cells of JS595 suggests that *c*DCE monooxygenase in JS666 is specialized to favor dichloroacetaldehyde rather than epoxide production from *c*DCE.

Chloroacetaldehyde and dichloroacetaldehyde react with DNA (45), tRNA (46), and proteins (47), forming adducts of uncertain toxicity (48). Neither dichloroacetaldehyde nor epoxide was detected in JS666 cultures that were grown continuously on *c*DCE. Dichloroacetaldehyde was transiently detected only during the brief lag phase following transfer and dilution of *c*DCE-grown cultures into fresh medium. The simultaneous induction studies showed that dichloroacetaldehyde and/or chloroacetaldehyde dehydrogenase has high constitutive activity that is upregulated to higher activities by growth on *c*DCE and DCA (Table 1). High activity of the dehydrogenase would protect the cells from the effects of toxic intermediates (49) and channel the carbon into a productive pathway. To our knowledge, this is the first report of a

productive pathway resulting from the P450-catalyzed conversion of an alkene to an aldehyde rather than an epoxide.

The rapid loss of activity in *E. coli* clones expressing the P450 complex is reminiscent of product toxicity to methane monooxygenase when oxygenated compounds are produced during transformation of TCE (epoxide) and chloroform (phosgene) (15, 50). For JS593 and JS595, the result is probably due to the toxicity of dichloroacetaldehyde. Chloroacetaldehyde (51) and dichloroacetaldehyde (52) react with free sulfhydryl groups, particularly with cysteine and glutathione. Cytochromes P450 have a critical cysteine ligand in the active site that binds and orients the heme moiety in the Cys pocket (53). Four cysteines act as the ligands that bind iron to ferredoxin/rubredoxin (54). When JS666 is grown on *c*DCE, a glutathione-*S*-transferase is upregulated over 100-fold (13). This, in addition to the high constitutive activity of chloroacetaldehyde/dichloroacetaldehyde dehydrogenase, would help to protect the cytochrome P450 complex from damage by dichloroacetaldehyde (55), but neither protection is available to the heterologously expressed proteins. Because dichloroacetaldehyde and chloroacetaldehyde are converted to hydrates in aqueous solutions (56), it was not possible to test the inactivation of the P450 enzyme with exogenous (di)chloroacetaldehyde. Addition of the hydrates had no effect on enzyme activity.

Conflicting carbon isotope fractionation results during *c*DCE degradation by JS666 suggested two different initial steps of *c*DCE degradation. Abe et al. (57) suggested the epoxidation of *c*DCE as the initial step of *c*DCE degradation by JS666 on the basis of the typical carbon isotope fractionation (−8.5‰) for epoxidation and a small chlorine isotope fractionation (−0.3‰). In contrast, the cleavage of a C—Cl bond was suggested by Jennings (58) to be the initial step of *c*DCE degradation by JS666 on the basis of the large carbon isotope fractionation (−17.4 to −22.4‰) during *c*DCE degradation. The cytochrome P450-catalyzed mechanism proposed here would be consistent with the latter results. Future clarification of the reaction mechanism and the factors controlling fractionation with purified enzymes will enable application of isotope fractionation to monitor aerobic *c*DCE degradation in the environment (59).

The presence of multiple pathways for *c*DCE degradation was suggested by two distinguishable modes of *c*DCE degradation by JS666 (13). One is faster and supports growth of JS666, whereas the other is slower, seems to be cometabolic, and probably involves some misrouting of intermediates. It seems likely that both pathways operate simultaneously in growing cells. Transcriptomics and proteomics indicate that *c*DCE causes upregulation of several genes that are candidates for encoding the competing initial reactions (13). Transcriptomics previously indicated that cyclohexanone monooxygenase is upregulated in JS666 grown on *c*DCE (13), and there is modest consumption of cyclohexanone by *c*DCE-grown cells (Table 1); however, the enzyme does not appear to be directly involved in *c*DCE degradation (65). Three lines of evidence support this conclusion. (i) There is no detectable oxygen uptake when DCA or *c*DCE is provided to cyclohexanone-grown cells, (ii) there is a 2- to 3-day lag period before resumption of growth upon switching between *c*DCE and cyclohexanone (in either direction) as growth substrates, and (iii) the simultaneous presence of *c*DCE and cyclohexanone in cultures of JS666 grown on *c*DCE reduces the rate of consumption of *c*DCE. *c*DCE degradation via dichloroacetaldehyde seems to be the major pathway, on the basis of the results presented here. The roles of cyclohexanone monooxygenase and other genes upregulated during growth on *c*DCE are under investigation.

The reductase and ferredoxin that constitute the electron transport chain for the *c*DCE monooxygenase are most closely related to the corresponding proteins involved in hexane and limonene monooxygenation in *Mycobacterium* sp. strain HXN-1500 (37). The cytochrome P450 from JS666 is slightly more closely related to a cytochrome P450 from *Mycobacterium austroafricanum* IFP 2173 that is upregulated in the presence of the branched alkane 2-ethyl hexyl nitrate. The HXN-1500 and IFP 2173 cytochrome P450 amino acid sequences are identical in 418/420 sites. The genes in JS666 are in the same orientation and order as those in HXN-1500. The context of the cytochrome P450 gene from *M. austroafricanum* is unknown. Cytochrome P450 alkane hydroxylases are among several alkane degradation systems (60) that catalyze the transformation of medium-chain-length alkanes (C_6 to C_{10}) to alkanols, which are further degraded to fatty acids by alcohol dehydrogenase (AlkJ), aldehyde dehydrogenase (AlkH), and acyl coenzyme A synthetase (AlkK). In JS666, putative *alkKJH* and pyrroloquinolinequinone (PQQ)-dependent dehydrogenase genes are located upstream of the cytochrome P450 monooxygenase genes, which is consistent with the growth of JS666 on heptane and octane (12). Mattes et al. suggest that the gene cluster was recently recruited from alkane-assimilating bacteria on the basis of the high G+C content, the association with several transposase genes, and the gene organization (12). Mattes et al. reported about 10-fold faster growth of JS666 on *c*DCE than on octane and JS595 transformed *c*DCE and DCA 4 to 6 times faster than octane (12). Purified enzymes catalyzed the transformation of octane to 1-octanol at a rate of 0.6 nmol min^{-1} mg^{-1} protein (38), only 10-fold faster than cells of JS595 (Table 3). The evidence suggests that although JS666 can still grow on *n*-alkanes, the enzymes and organism appear to be better adapted for growth on chlorinated alkenes/alkanes than on *n*-alkanes.

Instability and loss by JS666 of the ability to degrade *c*DCE under nonselective conditions (13), along with the lack of a clear organization of the genes involved, suggest that the system was recently assembled and sustained at the field site in response to contamination by *c*DCE. The most likely scenario for the assembly of the pathway would involve the recruitment and expression of the genes encoding the cytochrome P450 monooxygenase, which would allow the relatively common 1,2-dichloroethane-degrading bacteria (24, 31) to grow with *c*DCE as the sole source of carbon and energy. Genes of a 1,2-dichloroethane catabolic pathway might have been recruited for dichloroacetaldehyde degradation. Homologs of the cytochrome P450 monooxygenase seem to be readily available in soil, considering the widespread distribution of CYP153A alkane hydroxylases (61). Similar scenarios for assembly of chlorobenzene (62) and diphenylamine (63) degradation pathways by recruitment of genes from disparate pathways were strongly supported. Alternatively, a preexisting pathway for DCA degradation might employ a cytochrome P450 monooxygenase to catalyze the initial step. The presence of *c*DCE might then select for variants of the P450 that could catalyze the conversion of *c*DCE to dichloroacetaldehyde. Screening for cytochrome P450 monooxygenase genes in 1,2-dichloroethane-degrading bacteria will provide more insight about the evolution of the *c*DCE degradation pathway.

Uncertainty about the *c*DCE degradation pathway and intermediates has been a deterrent to the use of strain JS666 to reme-

diate sites contaminated with *c*DCE and to the assessment of *c*DCE degradation in the environment. The determination of the catabolic pathway and genes that encode the enzymes involved provides the basis to detect, predict, and enhance *c*DCE degradation in the environment as well as increase our understanding of bacterial evolution of catabolic pathways for synthetic chemicals.

ACKNOWLEDGMENTS

This work was supported by the Strategic Environmental Research and Development Program (SERDP ER-1557), Geosyntec Consultants, and the DuPont Corporate Remediation Group.

We thank Evan Cox (Geoxyntec Consultants) for patient management and support of this project. We thank Sarah Craven for many helpful discussions and assistance with clone expression. We thank Barbara Sherwood Lollar and Scott Mundle (Department of Geology, University of Toronto), Charlene Bayer (Georgia Tech Research Institute), and F. P. Guengerich (Vanderbilt University) for helpful discussions.

REFERENCES

1. **Agency for Toxic Substances and Disease Registry.** 2011. ATSDR 2011 substance priority list. Agency for Toxic Substances and Disease Registry, U.S. Department of Health and Human Services, Atlanta, GA.
2. **Maymó-Gatell X, Chien Y, Gossett JM, Zinder SH.** 1997. Isolation of a bacterium that reductively dechlorinates tetrachloroethene to ethene. Science **276**:1568–1571.
3. **Mohn WW, Tiedje JM.** 1992. Microbial reductive dehalogenation. Microbiol. Rev. **56**:482–507.
4. **Coleman NV, Mattes TE, Gossett JM, Spain JC.** 2002. Phylogenetic and kinetic diversity of aerobic vinyl chloride-assimilating bacteria from contaminated sites. Appl. Environ. Microbiol. **68**:6162–6171.
5. **Coleman NV, Spain JC.** 2003. Epoxyalkane:coenzyme M transferase in the ethene and vinyl chloride biodegradation pathways of *Mycobacterium* strain JS60. J. Bacteriol. **185**:5536–5545.
6. **Allen JR, Clark DD, Krum JG, Ensign SA.** 1999. A role for coenzyme M (2-mercaptoethanesulfonic acid) in a bacterial pathway of aliphatic epoxide carboxylation. Proc. Natl. Acad. Sci. U. S. A. **96**:8432–8437.
7. **Krum JG, Ensign SA.** 2001. Evidence that a linear megaplasmid encodes enzymes of aliphatic alkene and epoxide metabolism and coenzyme M (2-mercaptoethanesulfonate) biosynthesis in *Xanthobacter* strain Py2. J. Bacteriol. **183**:2172–2177.
8. **Mattes TE, Coleman NV, Spain JC, Gossett JM.** 2005. Physiological and molecular genetic analyses of vinyl chloride and ethene biodegradation in *Nocardioides* sp. strain JS614. Arch. Microbiol. **183**:95–106.
9. **Coleman NV, Mattes TE, Gossett JM, Spain JC.** 2002. Biodegradation of *cis*-dichloroethene as the sole carbon source by a β-proteobacterium. Appl. Environ. Microbiol. **68**:2726–2730.
10. **Fennell DE, Carroll AB, Gossett JM, Zinder SH.** 2001. Assessment of indigenous reductive dechlorinating potential at a TCE-contaminated site using microcosms, polymerase chain reaction analysis, and site data. Environ. Sci. Technol. **35**:1830–1839.
11. **Yang Y, McCarty PL.** 2002. Comparison between donor substrates for biologically enhanced tetrachloroethene DNAPL dissolution. Environ. Sci. Technol. **36**:3400–3404.
12. **Mattes TE, Alexander AK, Richardson PM, Munk AC, Han CS, Stothard P, Coleman NV.** 2008. The genome of *Polaromonas* sp. strain JS666: insights into the evolution of a hydrocarbon- and xenobiotic-degrading bacterium, and features of relevance to biotechnology. Appl. Environ. Microbiol. **74**:6405–6416.
13. **Jennings LK, Chartrand MMG, Lacrampe-Couloume G, Lollar BS, Spain JC, Gossett JM.** 2009. Proteomic and transcriptomic analyses reveal genes upregulated by *cis*-dichloroethene in *Polaromonas* sp. strain JS666. Appl. Environ. Microbiol. **75**:3733–3744.
14. **Ensign SA, Hyman MR, Arp DJ.** 1992. Cometabolic degradation of chlorinated alkenes by alkene monooxygenase in a propylene-grown *Xanthobacter* strain. Appl. Environ. Microbiol. **58**:3038–3046.
15. **Fox BG, Borneman JG, Wackett LP, Lipscomb JD.** 1990. Haloalkene oxidation by the soluble methane monooxygenase from *Methylosinus trichosporium* OB3b: mechanistic and environmental implications. Biochemistry **29**:6419–6427.
16. **Koziollek P, Bryniok D, Knackmuss H-J.** 1999. Ethene as an auxiliary substrate for the cooxidation of *cis*-1,2-ethene and vinyl chloride. Arch. Microbiol. **172**:240–246.
17. **Canada KA, Iwashita S, Shim H, Wood TK.** 2002. Directed evolution of toluene *ortho*-monooxygenase for enhanced 1-naphthol synthesis and chlorinated ethene degradation. J. Bacteriol. **184**:344–349.
18. **Rui L, Cao L, Chen W, Reardon KF, Wood TK.** 2004. Active site engineering of the epoxide hydrolase from *Agrobacterium radiobacter* AD1 to enhance aerobic mineralization of *cis*-1,2-dichloroethylene in cells expressing an evolved toluene *ortho*-monooxygenase. J. Biol. Chem. **279**: 46810–46817.
19. **Lee J, Cao L, Ow SY, Barrios-Llerena ME, Chen W, Wood TK, Wright PC.** 2006. Proteome changes after metabolic engineering to enhance aerobic mineralization of *cis*-1,2-dichloroethylene. J. Proteome Res. **5**:1388–1397.
20. **Guengerich FP.** 2007. Mechanisms of cytochrome P450 substrate oxidation: MiniReview. J. Biochem. Mol. Toxicol. **21**:163–168.
21. **Stanier RY, Palleroni NJ, Doudoroff M.** 1966. The aerobic pseudomonads: a taxonomic study. J. Gen. Microbiol. **43**:159–271.
22. **Gillam EMJ, Guo Z, Martin MV, Jenkins CM, Guengerich FP.** 1995. Expression of cytochrome P450 2D6 in *Escherichia coli*, purification, and spectral and catalytic characterization. Arch. Biochem. Biophys. **319**:540–550.
23. **van der Ploeg J, Smidt MP, Landa AS, Janssen DB.** 1994. Identification of chloroacetaldehyde dehydrogenase involved in 1,2-dichloroethane degradation. Appl. Environ. Microbiol. **60**:1599–1605.
24. **Janssen DB, Scheper A, Dijkhuizen L, Witholt B.** 1985. Degradation of halogenated aliphatic compounds by *Xanthobacter autotrophicus* GJ10. Appl. Environ. Microbiol. **49**:673–677.
25. **Carr CS, Hughes JB.** 1998. Enrichment of high-rate PCE dechlorination and comparative study of lactate, methanol, and hydrogen as electron donors to sustain activity. Environ. Sci. Technol. **32**:1817–1824.
26. **Bergmann JG, Sanik J, Jr.** 1957. Determination of trace amounts of chlorine in naphtha. Anal. Chem. **29**:241–242.
27. **Nakajima K, Ohta K, Mostefaoui TA, Chai W, Utsukihara T, Horiuchi CA, Murakami M.** 2007. Glyoxal sample preparation for high-performance liquid chromatographic detection of 2,4-dinitro-phenylhydrazone derivative: suppression of polymerization and mono-derivative formation by using methanol medium. J. Chromatogr. A **1161**:338–341.
28. **Wakasugi T, Miyakawa T, Suzuki F, Itsuno S, Ito K.** 1993. Preparation of dichloroacetaldehyde cyclic trimer and its depolymerization. Synth. Commun. **23**:1289–1294.
29. **Verce MF, Gunsch CK, Danko AS, Freedman DL.** 2002. Cometabolism of *cis*-1,2-dichloroethene by aerobic cultures grown on vinyl chloride as the primary substrate. Environ. Sci. Technol. **36**:2171–2177.
30. **Janssen DB, Grobben G, Hoekstra R, Oldenhuis R, Witholt B.** 1988. Degradation of trans-1,2-dichloroethene by mixed and pure cultures of methanotrophic bacteria. Appl. Microbiol. Biotechnol. **29**:392–399.
31. **Hage JC, Hartmans S.** 1999. Monooxygenase-mediated 1,2-dichloroethane degradation by *Pseudomonas* sp. strain DCA1. Appl. Environ. Microbiol. **65**: 2466–2470.
32. **Miller RE, Guengerich FP.** 1982. Oxidation of trichloroethylene by liver microsomal cytochrome P-450: evidence for chlorine migration in a transition state not involving trichloroethylene oxide. Biochemistry **21**:1090–1097.
33. **Smidt H, de Vos WM.** 2004. Anaerobic microbial dehalogenation. Annu. Rev. Microbiol. **58**:43–73.
34. **Stanier R.** 1947. Simultaneous adaptation: a new technique for the study of metabolic pathways. J. Bacteriol. **54**:339–348.
35. **Bhushan B, Trott S, Spain JC, Halasz A, Paquet L, Hawari J.** 2003. Biotransformation of hexahydro-1,3,5-trinitro-1,3,5-triazine (RDX) by a rabbit liver cytochrome P450: insight into the mechanism of RDX biodegradation by *Rhodococcus* sp. strain DN22. Appl. Environ. Microbiol. **69**: 1347–1351.
36. **Raag R, Swanson BA, Poulos TL, Ortiz de Montellano PR.** 1990. Formation, crystal structure, and rearrangement of a cytochrome $P\text{-}450_{cam}$ iron-phenyl complex. Biochemistry **29**:8119–8126.
37. **van Beilen JB, Holtackers R, Luscher D, Bauer U, Witholt B, Duetz WA.** 2005. Biocatalytic production of perillyl alcohol from limonene by using a novel *Mycobacterium* sp. cytochrome P450 alkane hydroxylase expressed in *Pseudomonas putida*. Appl. Environ. Microbiol. **71**:1737–1744.
38. **Scheps D, Honda Malca S, Hoffmann H, Nestl BM, Hauer B.** 2011. Regioselective ω-hydroxylation of medium-chain *n*-alkanes and primary

alcohols by CYP153 enzymes from *Mycobacterium marinum* and *Polaromonas* sp. strain JS666. Org. Biomol. Chem. **9**:6727–6733.
39. **van Beilen JB, Funhoff EG, van Loon A, Just A, Kaysser L, Bouza M, Holtackers R, Rothlisberger M, Li Z, Witholt B.** 2006. Cytochrome P450 alkane hydroxylases of the CYP153 family are common in alkane-degrading eubacteria lacking integral membrane alkane hydroxylases. Appl. Environ. Microbiol. **72**:59–65.
40. **Reineke W.** 2001. Aerobic and anaerobic biodegradation potentials of microorganisms, p 1–161. *In* Beek B (ed), The handbook of environmental chemistry: biodegradation and persistence, vol 2, part K. Springer-Verlag, Berlin, Germany.
41. **Stucki G, Krebser U, Leisinger T.** 1983. Bacterial growth on 1,2-dichloroethane. Experientia **39**:1271–1273.
42. **Meunier B, de Visser SP, Shaik S.** 2004. Mechanism of oxidation reactions catalyzed by cytochrome P450 enzymes. Chem. Rev. **104**:3947–3980.
43. **Liebler DC, Guengerich FP.** 1983. Olefin oxidation by cytochrome P-450: evidence for group migration in catalytic intermediates formed with vinylidene chloride and trans-1-phenyl-1-butene. Biochemistry **22**:5482–5489.
44. **de Visser SP, Kumar D, Shaik S.** 2004. How do aldehyde side products occur during alkene epoxidation by cytochrome P450? Theory reveals a state-specific multi-state scenario where the high-spin component leads to all side products. J. Inorg. Biochem. **98**:1183–1193.
45. **Kohwi Y, Kohwi-Shigematsu T.** 1988. Magnesium ion-dependent triple-helix structure formed by homopurine-homopyrimidine sequences in supercoiled plasmid DNA. Proc. Natl. Acad. Sci. U. S. A. **85**:3781–3785.
46. **Biemat J, Ciesiołka J, Gornicki P, Adamiak RW, Krzyzosiak W, Wiewiórowski M.** 1978. New observations concerning the chloroacetaldehyde reaction with some tRNA constituents. Stable intermediates, kinetics and selectivity of the reaction. Nucleic Acids Res. **5**:789–804.
47. **Bond T, Henriet O, Goslan EH, Parsons SA, Jefferson B.** 2009. Disinfection byproduct formation and fractionation behavior of natural organic matter surrogates. Environ. Sci. Technol. **43**:5982–5989.
48. **European Food Safety Authority.** 2006. Opinion of the Scientific Panel on Plant Health, Plant Protection Products and Their Residues on a request from EFSA related to the evaluation of dichlorvos in the context of Council Directive 91/414/EEC. EFSA J. **343**:1–45.
49. **Reineke W, Knackmuss H-J.** 1984. Microbial metabolism of haloaromatics: isolation and properties of a chlorobenzene-degrading bacterium. Appl. Environ. Microbiol. **47**:395–402.
50. **Alvarez-Cohen L, McCarty PL.** 1991. Product toxicity and cometabolic competitive inhibition modeling of chloroform and trichloroethylene transformation by methanotrophic resting cells. Appl. Environ. Microbiol. **57**:1031–1037.
51. **Schwerdt G, Kirchhoff A, Freudinger R, Wollny B, Benesic A, Gekle M.** 2007. Mesna or cysteine prevents chloroacetaldehyde-induced cell death of human proximal tubule cells. Pediatr. Nephrol. **22**:798–803.
52. **Liebler DC, Meredith MJ, Guengerich FP.** 1985. Formation of glutathione conjugates by reactive metabolites of vinylidene chloride in microsomes and isolated hepatocytes. Cancer Res. **45**:186–193.
53. **Hasemann CA, Kurumbail RG, Boddupalli SS, Peterson JA, Deisenhofer J.** 1995. Structure and function of cytochromes P450: a comparative analysis of three crystal structures. Structure **3**:41–62.
54. **van Beilen JB, Neuenschwander M, Smits THM, Roth C, Balada SB, Witholt B.** 2002. Rubredoxins involved in alkane oxidation. J. Bacteriol. **184**:1722–1732.
55. **Dowsley TF, Forkert P-G, Benesch LA, Bolton JL.** 1995. Reaction of glutathione with the electrophilic metabolites of 1,1-dichloroethylene. Chem. Biol. Interact. **95**:227–244.
56. **Elmore JD, Wong JL, Laumbach AD, Streips UN.** 1976. Vinyl chloride mutagenicity via the metabolites chlorooxirane and chloroacetaldehyde monomer hydrate. Biochim. Biophys. Acta **442**:405–419.
57. **Abe Y, Aravena R, Zopfi J, Shouakar-Stash O, Cox E, Roberts JD, Hunkeler D.** 2009. Carbon and chlorine isotope fractionation during aerobic oxidation and reductive dechlorination of vinyl chloride and *cis*-1,2-dichloroethene. Environ. Sci. Technol. **43**:101–107.
58. **Jennings LK.** 2009. Proteomic and transcriptomic analyses reveal genes upregulated by *cis-dichloroethylene* in *Polaromonas* JS666. Cornell University, Ithaca, NY.
59. **Schmidt KR, Augenstein T, Heidinger M, Ertl S, Tiehm A.** 2010. Aerobic biodegradation of *cis*-1,2-dichloroethene as sole carbon source: stable carbon isotope fractionation and growth characteristics. Chemosphere **78**:527–532.
60. **Van Beilen JB, Li Z, Duetz WA, Smits THM, Witholt B.** 2003. Diversity of alkane hydroxylase systems in the environment. Oil Gas Sci. Technol. **58**:427–440.
61. **Wang L, Wang W, Lai Q, Shao Z.** 2010. Gene diversity of CYP153A and AlkB alkane hydroxylases in oil-degrading bacteria isolated from the Atlantic Ocean. Environ. Microbiol. **12**:1230–1242.
62. **Muller TA, Werlen C, Spain J, van der Meer JR.** 2003. Evolution of a chlorobenzene degradative pathway among bacteria in a contaminated groundwater mediated by a genomic island in *Ralstonia.* Environ. Microbiol. **5**:163–173.
63. **Shin KA, Spain JC.** 2009. Pathway and evolutionary implications of diphenylamine biodegradation by *Burkholderia* sp. strain JS667. Appl. Environ. Microbiol. **75**:2694–2704.
64. **Chan WY, Wong M, Guthrie J, Savchenko AV, Yakunin AF, Pai EF, Edwards EA.** 2010. Sequence- and activity-based screening of microbial genomes for novel dehalogenases. Microb. Biotechnol. **3**:107–120.
65. **Alexander AK, Biedermann D, Fink MJ, Mihovilovic MD, Mattes TE.** 2012. Enantioselective oxidation by a cyclohexanone monooxygenase from the xenobiotic-degrading Polaromonas sp. strain JS666. J. Mol. Catal. B Enzym. **78**:105–110.